International Journal of Pharmaceutics 393 (2010) 203–211

Contents lists available at ScienceDirect

International Journal of Pharmaceutics

journal homepage: www.elsevier.com/locate/ijpharm

Pharmaceutical Nanotechnology

The efficacy and safety of bufadienolides-loaded nanostructured lipid carriers

Fang Li[a], Yan Weng[a], Lihui Wang[b], Haibing He[a], Jingyu Yang[b], Xing Tang[a,*]

[a] Department of Pharmaceutics, Shenyang Pharmaceutical University, No. 103, Wenhua Road, Shenyang 110016, PR China
[b] Department of Pharmacology, Shenyang Pharmaceutical University, Shenyang 110016, PR China

ARTICLE INFO

Article history:
Received 10 February 2010
Received in revised form 25 March 2010
Accepted 5 April 2010
Available online 10 April 2010

Keywords:
Bufadienolides
Nanostructured lipid carriers
Cytotoxicity
Pharmacokinetics
Biodistribution
Antitumor activity

ABSTRACT

Bufadienolides-loaded nanostructured lipid carriers (BU-NLC) were prepared for parenteral application using glyceryl monostearate as solid core, medium-chain triglyceride and oleic acid as liquid lipid material, and Lipoid E-80®, sodium deoxycholate and pluronic F68 as stabilizers. In this study, the *in vitro* cytotoxicity, pharmacokinetics, biodistribution, antitumor efficacy and safety of BU-NLC were evaluated. Against human astrocytoma cell line (U87-MG) and human gastric carcinoma cell line (HGC-27) BU-NLC exhibited cytotoxicity that was similar to that of the free drug, and superior to that of the commercially available fluorouracil injection. BU-NLC exhibited a linear pharmacokinetic behavior at doses ranging from 0.25 to 1.0 mg/kg. The improved pharmacokinetic profile of bufadienolides when formulated in BU-NLC resulted in a higher plasma concentration and lower clearance after intravenous administration compared with bufadienolides solution (BU-S). A biodistribution study indicated that bufadienolides were mainly distributed in the lung, spleen, brain and kidney, and the longest retention was observed in the brain. A sarcoma-180 tumor model further confirmed the advantages of BU-NLC versus BU-S. Hemolysis and acute toxicity investigations showed that BU-NLC was safe when given by intravenous injection with reduced toxicity. In conclusion, the NLC system is a promising approach for the intravenous delivery of bufadienolides.

1. Introduction

The therapeutic properties of toad venom, a traditional Chinese medicine, have been exploited for thousands of years in China. The principal biologically active components of toad venom are bufadienolides, a class of C-24 steroids with a characteristic α-pyrone ring at C-17 (Krenn and Kopp, 1998; Steyn and van Heerden, 1998). Bufadienolides exhibit a range of biological activities, such as antineoplastic effects, stimulation of myocardial contraction and blood pressure, anti-inflammatory effects, respiration effects and pain relief. The major bufadienolides from toad venom include bufalin (B), cinobufagin (C) and resibufogenin (R), each being significantly cytotoxic to cancer cells (Kamano et al., 2002; Yeh et al., 2003). These bufadienolides are considered to be the most toxic components of toad venom and they are poorly water-soluble which makes the formulation of bufadienolides rather challenging.

In the present study, the bioactive pure bufadienolides were isolated from Chan Su, the Chinese toad, in the form of round, smooth, dark brown discs. Bufadienolides (purity 95%) were highly lipophilic with a mass ratio of 2:3:5 for B, C and R, respectively. Recently it was found that compound C was readily degradable by rat plasma esterase. Encapsulation of bufadienolides in several intravenous dosage forms, such as a nanoemulsion, submicroemulsion and liposomes (Li et al., 2008, 2009), failed to improve the chemical stability of C. Attempts has been made to load the bufadienolides into nanostructured lipid carriers (NLCs). NLCs are improved forms of solid lipid nanoparticles (SLN) (Müller et al., 2007). The solid core of NLCs, unlike the fluid core of liposomes and emulsions, offer the advantages of biocompatibility, and improved drug loading capacity and release properties (Joshi and Müller, 2009). The chemical stability of C in rat plasma is greatly enhanced when encapsulated in nanostructured lipid carriers (Li et al., 2010).

Encapsulation of biologically active agents in NLCs can dramatically enhance their activity by acting as a drug reservoir. A few reports on the *in vivo* behaviour of SLN have been published showing that nanoparticle formulations reduce the cardiotoxic side effects of doxorubicin in Wistar rats and prolong the metabolism of doxorubicin (Fundarò et al., 2000; Miglietta et al., 2000). NLCs are removed from the circulation by a mononuclear phagocyte system, largely in the liver and spleen, or by extravasation in areas where the vascular membrane is more permeable, such as sites of tumors, inflammation and infection. This will increase the accumulation of bufadienolides in tumor tissues and reduce the cardiac damage associated with these agents. In addition, it is well known that NLCs are less cytotoxic than polymeric nanoparticles (Müller et al., 1997) and, therefore, NLCs were selected as an alternative carrier for bufadienolides in the present study.

* Corresponding author. Tel.: +86 24 23986343; fax: +86 24 23911736.
E-mail address: tangpharm@yahoo.com.cn (X. Tang).

0378-5173/$ – see front matter © 2010 Elsevier B.V. All rights reserved.
doi:10.1016/j.ijpharm.2010.04.005

The objective of this study was to evaluate the *in vitro* cytotoxicity of bufadienolides-loaded nanostructured lipid carriers (BU-NLC) and their fate after parenteral delivery *in vivo*. The *in vitro* cytotoxicity of BU-NLC was examined by a microculture tetrazolium (MTT) colorimetric assay using two tumor cell lines, a human astrocytoma cell line (U87-MG) and a human gastric carcinoma cell line (HGC-27). The pharmacokinetics, biodistribution and therapeutic efficacy of BU-NLC were investigated for the first time. Male Kunming mice with a sarcoma-180 tumor were used to study the *in vivo* antitumor activity of BU-NLC. The hemolytic activity of BU-NLC was evaluated by using the method proposed by the 2005 edition of the *China Pharmacopoeia*. Since bufadienolides have been reported to produce cardiac dysrhythmias and other cardiovascular effects, the acute toxicity of BU-NLC was also investigated in mice in comparison with bufadienolides solution (BU-S).

2. Materials and methods

2.1. Materials

Lipoid E-80®, oleic acid (OA) and medium-chain triglyceride (MCT) were purchased from Lipoid (Ludwigshafen, Germany). Glyceryl monostearate (GM), pluronic F68 and sodium deoxycholate (SDC) were obtained from Tianjin Bodi Chemicals Co., Ltd. (Tianjin, China), BASF AG (Ludwigshafen, Germany) and Sigma–Aldrich (Steinheim, Germany), respectively. The human astrocytoma cell line (U87-MG) and the human gastric carcinoma cell line (HGC-27) were obtained from American Type Culture Collection (Manassas, American). Fluorouracil injection and a lyophilized-injection of cyclophosphamide were obtained from Jiangsu Hengrui Medicine Co., Ltd. (Jiangsu, China) and Shanghai Xudong Haipu Pharmaceutical Co., Ltd. (Shanghai, China), respectively. All other chemicals were of analytical or chromatographic grade.

2.2. Animals

All animals used in this study were obtained from the Experiment Animal Center (Shenyang Pharmaceutical University, Shenyang, China). The experimental procedures complied with the University Animal Ethics Committee Guidelines.

2.3. Preparation of formulations

Bufadienolides-loaded nanostructured lipid carriers (BU-NLC) were prepared by a modified melt-emulsification and ultrasonic method. Briefly, GM (1.8 g), MCT (0.75 g) and OA (0.45 g) were heated together in a water bath at 75 °C. Then, the bufadienolides were dissolved in the melted lipid phase under stirring to form a lipid phase. Lipoid E-80® (1.5 g), pluronic F68 (1.0 g) and SDC (0.25 g) were dissolved in 80 mL distilled water at 75 °C as the aqueous phases. The aqueous phase was then dispersed in the lipid phase under magnetic stirring at the same temperature. The obtained primary emulsion was ultrasonicated using a probe sonication instrument (Sonics & Material Vibra Cell, 750 W, 20 kHz) at 30% amplification for 10 min with a 3-s pulse-on period and a 1-s pulse-off period. The nanoemulsion (O/W) obtained was cooled in an ice bath under magnetic stirring followed by dilution to 100 mL with distilled water. Finally, the resultant NLCs were filtered through a 0.22 μm membrane.

The bufadienolides solution (BU-S) was prepared by dissolving bufadienolides in propylene glycol under ultrasonication. Then, the propylene glycol solution was diluted to a concentration of 20% with distilled water to give a 0.5 mg/mL solution of bufadienolides for pharmacokinetic, tissue distribution and acute toxicity studies.

2.4. In vitro cytotoxicity assay

The cytotoxic effects of bufadienolides dissolved in DMSO (BU-D), commercially available fluorouracil injection (Fu) and BU-NLC on U87-MG and HGC-27 cell lines were determined using an MTT assay. Tumor cells were seeded in 96-well plates and incubated at 37 °C for 24 h. Cells were then treated with BU-D and BU-NLC (at concentrations of 0.016, 0.08, 0.4, 2, and 10 μg/mL) for 48, 72 and 96 h, respectively. The cytotoxicity of Fu was evaluated over the drug concentration range from 0.1 to 100 μg/mL. Then, 3-(4, 5-dimethylthiazol-2-yl)-2, 5-diphenyl-tetrazolium bromide (MTT, 2.5 mg/mL in PBS) was added to each well and cells were incubated at 37 °C for 4 h. The formazan produced was dissolved in DMSO. The absorbance of each well was measured using a Microplate Reader at a wavelength of 492 nm.

2.5. Pharmacokinetic study

Twenty-four Wistar rats (200–250 g) were randomly divided into four groups, each of six rats (a, b, c and d; equal numbers of males and females in each group). Group a, b and c were given BU-NLC at bufadienolides doses of 0.25, 0.5 and 1.0 mg/kg via the femoral vein while the group d was given BU-S at a bufadienolides dose of 1.0 mg/kg. Blood samples were taken from the terminal retro-orbital region at 0 (predose), 5, 10, 15, 20, 30, 40, 50, 60, 90 and 120 min after administration and transferred to heparinized Eppendorf tubes. Then, the heparinized blood was centrifuged for 10 min at 4000 rpm, and the plasma obtained was stored frozen at −70 °C until analysis.

2.6. Tissue distribution study

In the tissue distribution study, 60 Kunming mice (20 ± 2 g) were divided into two groups of 30 mice (equal numbers of males and females in each group). BU-NLC and BU-S were given intravenously via the tail vein at a dose of 1.5 mg bufadienolides/kg body weight. After injection, 6 mice (3 male and 3 female) were sacrificed at 2, 5, 15, 30 and 240 min for each group. Then, the heart, liver, spleen, lung, kidney and brain of each mouse were rapidly removed following blood collection, and immediately washed with normal saline, wiped with filter paper, weighed and stored at −70 °C.

2.7. In vivo antitumor activity study

Sixty Kunming mice (male, 18–22 g), randomly divided into six groups ($n = 10$), were injected subcutaneously with sarcoma-180 (S180) tumor cells (5×10^6 cells/0.2 mL) in the right flank. This day was set as day 0. After inoculation for 24 h, 0.2 mL BU-NLC at three dose levels (0.25, 0.5 and 1.0 mg/kg bufadienolides) and 0.2 mL BU-S at a high dose of 1.0 mg/kg were administered via the tail vein for continuous 7 days. At the same time, the negative control group (N.C.) was treated with 0.2 mL normal saline. Mice given a commercially available lyophilized-injection of cyclophosphamide (2.5 mg/kg/day) were used as the positive control group (P.C.).

The mice were dissected on the 8th day post-inoculation and the tumors, thymuses and spleens were excised. Solid tumors were harvested for gross macroscopic observation and subjected to morphological investigation using an electronic transmission microscope (JEM-1200, JEOL, Tokyo, Japan). The index of the thymus (I.T.) was measured using the ratio of the thymus weight (mg) to body weight (g). The index of the spleen (I.S.) was measured using the ratio of the spleen weight (mg) to body weight (g). Values are means ± SD of 10 mice. The excised tissues were weighed, and the

inhibition rate of tumor growth (I.R.) was calculated as follows:

$$\text{I.R.}(\%) = \frac{A - B}{A} \times 100$$

where A is the average tumor weight of the negative control group, B is the average tumor weight of the test group.

2.8. Safety test of BU-NLC

2.8.1. Hemolysis assay

Erythrocytes were isolated from fresh whole rabbit blood. Different amounts of sample solution, 0.1, 0.2, 0.3, 0.4 and 0.5 mL, were added to five tubes along with 2.5 mL 2% erythrocyte dispersion. Then, normal saline was added to every tube to obtain a final volume of 5 mL. Positive and negative controls were prepared by the addition of water (2.5 mL) and normal saline (2.5 mL) to 2.5 mL samples of 2% erythrocyte dispersion. Following incubation at 37 °C for 1 h, the samples were centrifuged at 2000 rpm for 10 min and the amount of released hemoglobin was measured spectrophotometrically at a wavelength of 576 nm (UV 4802H, Unico, Dayton, USA). Optical microscopy (DMBA 450, Motic, Xiamen, China) was also used to see if there were any abnormalities in the blood cells after incubation. The hemolysis rate was calculated from the following equation:

$$\text{Hemolysis rate}(\%) = \frac{A_s - A_0}{A_{100} - A_0} \times 100$$

where A_s is the absorbance of the sample, A_0 is the absorbance of the negative control and A_{100} is the absorbance of the positive control.

2.8.2. Acute toxicity study

Kunming mice (equal numbers of males and females, 18–22 g) were housed under normal conditions with free access to food and water. Five male and five female mice per dosing group ($n = 10$) were used. BU-NLC and BU-S were injected via the tail vein at doses of 1.32, 1.66, 2.07, 2.59, 3.24 and 4.05 mg/kg. Dose-related toxic effects were observed immediately, 4 h post-injection and then daily for 2 weeks in all groups, and the number of mice surviving was recorded. The median lethal dose (LD_{50}) was calculated using the Bliss method.

2.9. Data analysis

All the data obtained on BU-NLC and BU-S were analyzed statistically by one-way analysis of variance and Student's t-test. In all cases, a value of $p < 0.05$ was considered to represent statistical significance.

3. Results

3.1. Characterization of BU-NLC

The BU-NLC was prepared by a modified melt-emulsification ultrasonic technique (Li et al., 2010). The particle size distribution and the range of zeta potential of BU-NLC were 104.1 ± 51.2 nm and −15 to −20 mV, respectively. The entrapment efficiency (EE) of BU-NLC was evaluated by the microdialysis technique. The entrapment efficiencies (EEs) of B, C and R in BU-NLC were 87.4%, 93.7% and 95.6%, respectively. As expected from the solid state of the core lipid, the encapsulation of ingredients into the lipid matrix offered protection against compound degradation (Schubert et al., 2006). In the enzymolysis study, the chemical stability of C in BU-NLC was enhanced by being encapsulated in particles of NLC and adjusting the pH of the surrounding environment to 7.0. Using DSC analysis and X-ray diffraction, the drug was found to be in an amorphous state in the NLC particles. The *in vitro* drug release behavior fitted the Weibull distribution closely and exhibited a biphasic drug release pattern.

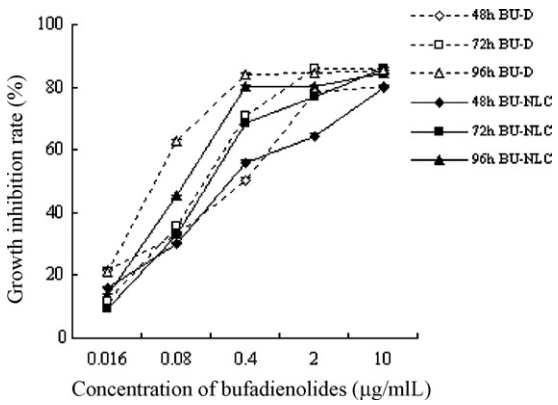

Fig. 1. Time-dependent inhibition rates of BU-NLC and BU-D in the HGC-27 cell line *in vitro*.

3.2. Cytotoxicity evaluation

Figs. 1 and 2 show the inhibition rates of free bufadienolides dissolved in DMSO (BU-D) and BU-NLC in HGC-27 and U87-MG cell lines *in vitro* after 48, 72 and 96 h incubation period. Both formulations showed a similar time-dependent and concentration-dependent behavior in the two cell lines. BU-D, at a concentration of 2 μg/mL, caused a strong inhibition of HGC-27 cell growth after 48, 72 and 96 h exposure (78.26 ± 0.33%, 85.92 ± 0.30% and 84.47 ± 0.51%). In case of BU-NLC, the HGC-27 cell inhibition rates were 64.45 ± 0.69%, 76.95 ± 0.25% and 80.42 ± 0.53%. BU-D showed a greater inhibitory effect in the HGC-27 cell line below 2 μg/mL. There was no significant difference between the two formulations at the concentration of 10 μg/mL. However, for the U87-MG cell, the viability was significantly decreased following treatment with BU-NLC compared with the cells after incubation with BU-D at the highest concentration. The inhibition rates of BU-NLC and BU-D with10 μg/mL bufadienolides were 84.47 ± 0.30% and 61.06 ± 0.32% after 48 h, 88.55 ± 0.13% and 65.43 ± 1.35% after 72 h, 88.59 ± 0.47% and 86.14 ± 0.09% after 96 h, respectively (Fig. 2).

The half maximal inhibitory concentration (IC_{50}) values are presented in Table 1. The effects of both BU-NLC and BU-D in the two cell lines were superior to that of Fu. In HGC-27 cells, the cytotoxicity of BU-NLC was lower than that of BU-D after 48, 72 and 96 h

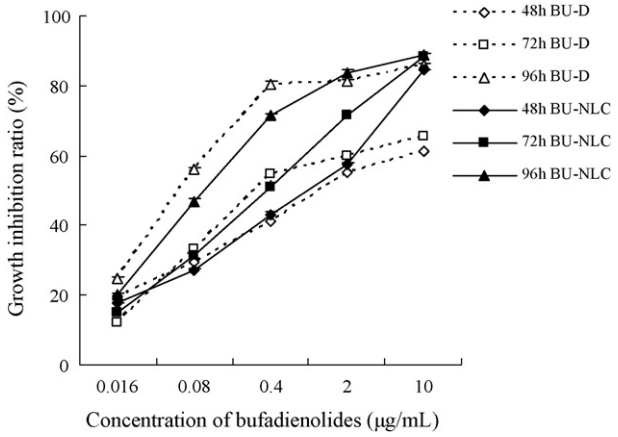

Fig. 2. Time-dependent inhibition rates of BU-NLC and BU-D in the U87-MG cell line *in vitro*.

Table 1
IC_{50} of BU-NLC, BU-D and fluorouracil injection (Fu) on the growth of HGC-27 and U87-MG cell lines after 48, 72 and 96 h exposure.

Formulations	IC_{50} of HGC-27 (μg/mL)			IC_{50} of U87-MG (μg/mL)		
	48 h	72 h	96 h	48 h	72 h	96 h
BU-NLC	0.50 ± 0.07	0.19 ± 0.04	0.10 ± 0.01	0.84 ± 0.10	0.43 ± 0.07	0.10 ± 0.02
BU-D	0.29 ± 0.02	0.15 ± 0.01	0.06 ± 0.001	1.30 ± 0.10	0.40 ± 0.12	0.07 ± 0.02
Fu	>100	11.24 ± 1.24	5.39 ± 0.62	53.06 ± 2.75	17.33 ± 2.30	4.50 ± 0.51

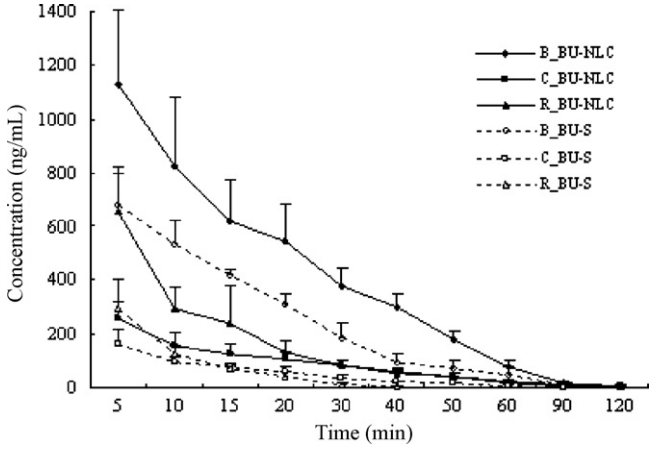

Fig. 3. The plasma concentration–time profiles of B, C and R after intravenous administration of BU-NLC and BU-S in rats ($n = 6$).

exposure. It is interesting that BU-NLC exhibited a faster onset of cytotoxicity in U87-MG cells. The cytotoxicity of BU-NLC was higher than that of BU-D at 48 h. However, at 72 and 96 h, the amount of bufadienolides required to achieve the IC_{50} value was higher with loaded NLC than with free drug. The cytotoxicity of BU-NLC in U87-MG cell line was time-dependent.

3.3. Pharmacokinetics study

In this study, the intravenous administration of BU-NLC to rats at doses of 0.25, 0.5 and 1.0 mg/kg was investigated in detail. A non-compartment model was used to calculate the pharmacokinetic parameters using drug and statistics (DAS) version 2.0 software (Mathematical Pharmacology Professional Committee of China, Shanghai, China). In Table 2, the C_{max} and $AUC_{(0-\infty)}$ of B, C and R in BU-NLC increased in proportion to the concentration. A dose-proportionality study suggested that there was a good correlation between the AUC and the dose. For B, C and R, the relationships were $AUC_{(0-\infty)} = 2.80\,Dose - 71.84$, $AUC_{(0-\infty)} = 0.39\,Dose - 9.12$ and $AUC_{(0-\infty)} = 0.47\,Dose - 6.76$, and the R^2 of the regression was 0.9984, 0.9986 and 0.9990, respectively. Using Student's *t*-test, at the three doses of 0.25, 0.5 and 1.0 mg/kg, no statistically significant difference was found in the pharmacokinetic parameters ($t_{1/2}$, CL and V_{ss}) of B, C and R, suggesting the linear pharmacokinetic behavior of bufadienolides after intravenous administration of BU-NLC over the above dose range.

The plasma pharmacokinetics profiles of BU-NLC and BU-S at a dose of 1.0 mg/kg bufadienolides is shown in Fig. 3. The pharmacokinetic profiles of the three bufadienolides were best described by a two-compartment model with a weighting factor = $1/c^2$, reflecting rapid elimination from blood. For both formulations, no bufadienolides could be detected 120 min after dosing. B, C and R are all highly lipophilic, which may be the major reason for their observed pharmacokinetic properties. The overall plasma concentrations of B, C and R following administration of BU-NLC were slightly higher than those of BU-S. In the animals injected with BU-NLC, the plasma concentrations of B, C and R declined with a CL of approximately 0.42 ± 0.06, 2.78 ± 0.34 and 2.23 ± 0.36 L/h/kg, while the corresponding values were 0.76 ± 0.14, 5.44 ± 1.40 and 6.96 ± 2.90 L/h/kg after administration of BU-S. For BU-NLC, the $AUC_{(0-\infty)}$ of B, C and R was 1.87-, 1.96- and 2.84-fold higher than that of BU-S, and the peak plasma concentrations (C_{max}) were also increased ($P < 0.05$). The results of the pharmacokinetics study showed that the pharmacokinetic behavior of B, C and R after administration of the BU-NLC preparation was significantly different from that of BU-S.

3.4. Tissue distribution

The organ concentrations of B, C and R following administration of BU-NLC and BU-S are shown in Fig. 4. At 2 min after administration of BU-NLC and BU-S, the concentrations of B, C and R in tissues all reached a maximum and then decreased rapidly. Bufadienolides were detectable at 15 min and almost undetectable at 30 min in all the examined tissues (except brain) for both BU-NLC and BU-S, which indicated that bufadienolides were distributed rapidly and there was no evident long-term accumulation of bufadienolides in tissues. As shown in Fig. 4, the distribution behavior of B, C and R in each tissue depended on the drug carrier. The total concentrations of bufadienolides from BU-NLC were highest in lung, followed by spleen, brain, kidney, heart and liver. It was noteworthy that at each time point the concentrations of bufadienolides in heart were higher for BU-S than for BU-NLC. For example, the concentrations of B, C and R in heart were 239.86 ± 61.17, 543.32 ± 152.80 and 415.26 ± 87.23 ng/g for BU-NLC, while the corresponding values were 371.89 ± 60.80, 941.84 ± 183.62 and 1001.85 ± 284.87 ng/g for BU-S at 2 min. The concentration of bufadienolides in heart contributed to their cardioactivity (Abdel-Rahman et al., 2010). Compared with other drugs, the three bufadienolides showed a relative higher accumulation in brain. In brain, bufadienolides were metabolized slowly and 4 h after intravenous administration, B and C were still detectable.

During this period, the lowest bufadienolides concentrations for BU-NLC and BU-S were all observed in liver. In particular, the mean concentrations of C for BU-NLC and BU-S were all below 50 ng/g. This was quite different from their concentrations in other tissues. This phenomenon may be due to their chemical structures and the metabolic action of the liver (Toma et al., 1991; Zhang et al., 1991), whereby bufadienolides underwent intensive metabolism and elimination in the liver. The uptake by the reticuloendothelial system, including the spleen and liver, was observed to be higher for BU-NLC compared with BU-S. Up to 15 min, R in spleen and B in lung were detectable after administration of BU-NLC. B and C from BU-NLC were also detectable in liver at 30 min. Thus, it can be concluded that incorporation into NLC prolonged the retention of bufadienolides within the systemic circulation. The *in vivo* behavior of the nanoparticles was similar to that widely reported in the literature for various colloidal systems (Junzo et al., 2004; Couvreur and Vauthier, 2006). This indicated a possible enhancement of the therapeutic index of the drug when administered as an NLC formulation. However, this needs further investigation.

Table 2
Pharmacokinetic parameters of B, C and R after intravenous administration of BU-NLC and BU-S in rats.

Parameters		Dose (μg/kg)	$AUC_{(0-\infty)}$ (μg h/L)	C_{max} (μg/L)	$t_{1/2}$ (h)	$MRT_{0-\infty}$ (h)	V_{ss} (L/kg)	CL (L/h/kg)
B		54	72.61 ± 6.85	190.16 ± 35.09	0.23 ± 0.07	0.28 ± 0.04	0.25 ± 0.08	0.76 ± 0.07
	BU-NLC	108	241.33 ± 25.98	420.73 ± 70.97	0.27 ± 0.07	0.37 ± 0.04	0.18 ± 0.04	0.46 ± 0.05
		216	530.22 ± 70.08	1144.99 ± 253.79	0.24 ± 0.08	0.37 ± 0.07	0.14 ± 0.04	0.42 ± 0.06
	BU-S	216	283.56 ± 37.43	687.12 ± 138.62	0.22 ± 0.01	0.30 ± 0.04	0.24 ± 0.03	0.78 ± 0.12
C		80	20.92 ± 5.02	58.02 ± 19.97	0.24 ± 0.02	0.30 ± 0.04	1.37 ± 0.26	3.96 ± 0.78
	BU-NLC	160	55.69 ± 4.00	97.72 ± 24.75	0.30 ± 0.09	0.41 ± 0.10	1.21 ± 0.32	2.87 ± 0.19
		320	115.77 ± 12.98	255.67 ± 60.31	0.28 ± 0.07	0.40 ± 0.06	1.12 ± 0.28	2.78 ± 0.34
	BU-S	320	59.20 ± 12.58	162.14 ± 55.88	0.20 ± 0.03	0.29 ± 0.04	1.63 ± 0.44	5.62 ± 1.43
R		116	49.72 ± 8.70	126.17 ± 45.97	0.36 ± 0.17	0.42 ± 0.15	1.19 ± 0.50	2.39 ± 0.42
	BU-NLC	232	99.33 ± 9.55	230.74 ± 79.50	0.30 ± 0.07	0.36 ± 0.08	1.02 ± 0.27	2.35 ± 0.22
		464	212.29 ± 35.73	656.29 ± 145.40	0.36 ± 0.12	0.30 ± 0.05	1.15 ± 0.29	2.23 ± 0.36
	BU-S	464	74.80 ± 25.95	297.21 ± 107.27	0.10 ± 0.01	0.13 ± 0.02	0.97 ± 0.40	6.96 ± 2.90

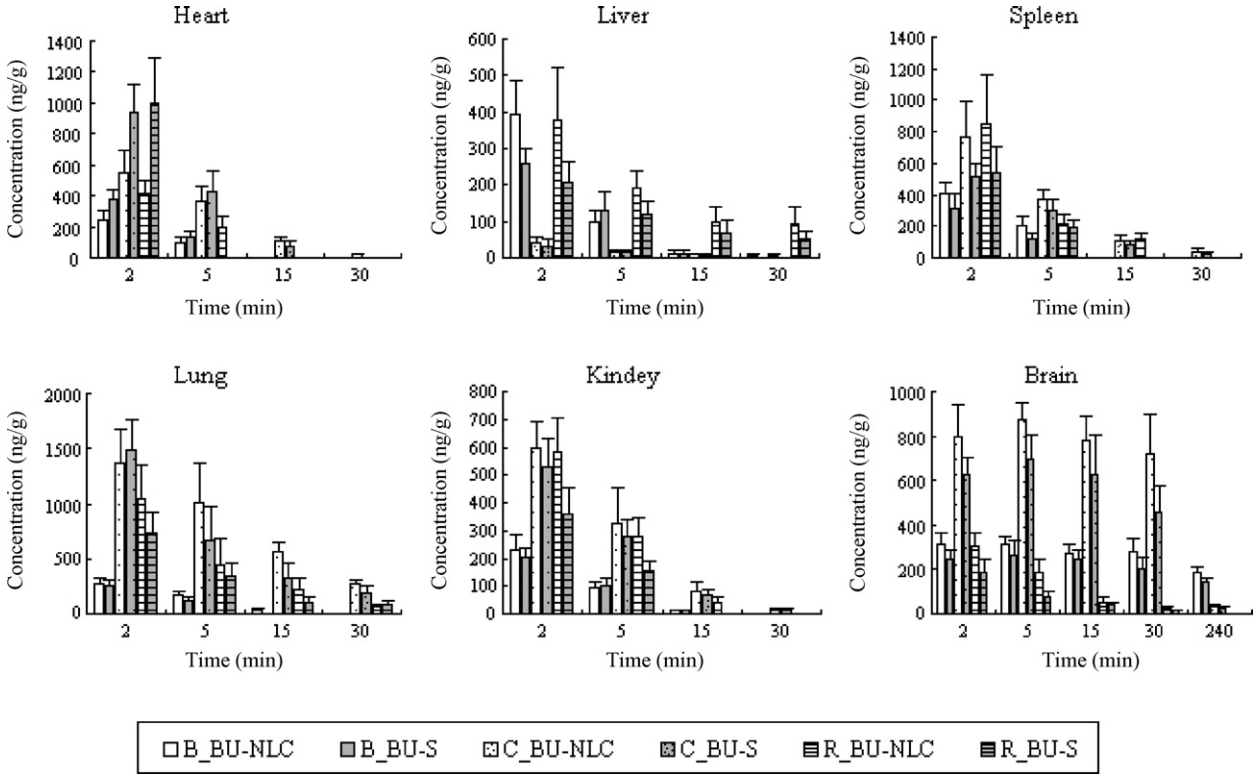

Fig. 4. Concentrations of B, C and R (ng/g organ) in mice after intravenous administration of BU-NLC and BU-S.

3.5. *In vivo* antitumor activity study

The *in vivo* antitumor effect of BU-NLC was assessed using S180-tumor-bearing mice as a model. Fig. 5 shows the variation in the mean body weight of the mice injected with different formulations. Compared with the negative control group, the mice experienced a slight weight loss in the 7 days after the administration of either BU-NLC or BU-S. Table 3 lists the effects of BU-NLC and BU-S on the growth of S180-tumor-bearing mice. All groups, apart from the negative control group, exhibited significant tumor inhibition (inhibition rate more than 30%). At doses of 0.25, 0.5 and 1.0 mg/kg/d BU-NLC, the tumor inhibition rates were 39.84%, 50.80% and 67.12%, respectively. More interestingly, the group treated with BU-S at the dose of 1.0 mg/kg/d showed a lower

Table 3
Effects of BU-NLC and BU-S on the growth of S180-tumor-bearing mice.

Group	Dose (mg/kg/d)	Body weight after being treated (g)	Weight of tumor (g)	I.R. (%)	I.T.	I.S.
N.C.	–	28.02 ± 1.97	0.81 ± 0.20	–	2.97 ± 0.59	6.99 ± 0.96
P.C.	2.50	25.00 ± 1.76	0.37 ± 0.09	54.15	2.48 ± 0.56	4.88 ± 1.06
hBU-NLC	1.00	26.37 ± 1.69	0.27 ± 0.09	67.12	2.78 ± 0.33	6.61 ± 1.80
mBU-NLC	0.50	26.06 ± 1.96	0.40 ± 0.15	50.80	3.24 ± 0.91	7.32 ± 1.25
lBU-NLC	0.25	27.06 ± 1.96	0.49 ± 0.17	39.84	3.43 ± 0.59	6.44 ± 1.77
BU-S	1.00	24.43 ± 2.48	0.51 ± 0.09	36.93	2.95 ± 0.70	6.52 ± 1.60

N.C.: mice treated with normal saline; P.C.: mice treated with a clinically available lyophilized-injection of cyclophosphamide; lBU-NLC, mBU-NLC and hBU-NLC: mice treated with BU-NLC at three dose levels (0.25, 0.5 and 1.0 mg/kg/d); BU-S: mice treated with BU-S at the dose of 1.0 mg/kg/d.

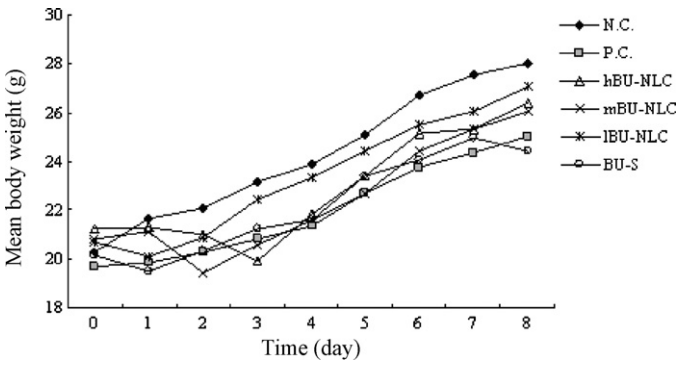

Fig. 5. Changes in the mean body weight of S180-tumor-bearing mice in each group.

inhibition rate (36.93%) which was equal to that of the group treated with BU-NLC at the dose of 0.25 mg/kg/d. The drug, bufadienolides in either BU-NLC or BU-S, could markedly increase the thymus and spleen index in S180-tumor-bearing mice. The P.C. group considerably reduced the thymus and spleen index in S180-tumor-bearing mice, whereas it exhibited a high inhibition (54.15%) at a dose of 2.5 mg/kg/d.

Fig. 6 shows an image of the excised tumors from each group, which provides a direct visual representation of the tumor-suppression effect. In contrast, in the groups treated with BU-NLC or cyclophosphamide, the excised tumors had a much smaller size with a much more regular shape, suggesting that the tumor growth was markedly suppressed. To determine the antitumor mechanisms, the morphological changes were observed in S180-tumor-bearing mice in each group (Fig. 7). In Fig. 7(D), there is the formation of an apoptotic body in this picture of the P.C. group. The treatment with either BU-NLC or BU-S to inhibit the growth rate of tumor cells was further supported by pycnosis of the nucleus, an increase in heterochromatin secretion, karyorrhexis, and apoptosis as shown by the transmission electron microscope observations in Fig. 7(B and C).

3.6. Safety

The safety of administered agents can be evaluated by the red cell haemolysis assay. The hemolytic potential of BU-NLC was evaluated to ensure its hemocompatibility. In the present study, the BU-NLC was diluted with 5% glucose injection solution to give different lipid concentrations. As shown in Table 4, when the sample volumes were 0.1, 0.2, 0.3, 0.4 and 0.5 mL, the hemolysis rates of BU-NLC at a lipid concentration of 3.0 mg/mL were $3.51 \pm 0.73\%$, $5.77 \pm 0.86\%$, $15.83 \pm 2.76\%$, $36.86 \pm 3.87\%$ and $84.70 \pm 5.38\%$, respectively. When BU-NLC was further diluted to a lipid concentration of 1.2 mg/mL, the hemolysis rates were all below 5% for each test sample. Optical microscopy studies confirmed the intactness of the blood cells after incubation with the BU-NLC at a lipid concentration of 1.2 mg/mL, thereby proving its safety (Fig. 8). This result also acted as a guide for the administration of BU-NLC in clinical studies.

The aim of the encapsulation of bufadienolides, lowering the risk of toxicity, was distinctly different from that of other therapeutic agents. Thus, the LD_{50} of BU-NLC and BU-S was determined to compare their acute toxicity. The LD_{50} and 95% confidence limits of BU-S was 2.31 and 2.12–2.52 mg/kg, respectively. The corresponding LD_{50} of BU-NLC was 2.95 mg/kg, and the 95% confidence limits were found to fall within the range 2.65–3.28 mg/kg, The LD_{50} of BU-NLC was 1.28-fold higher than that of BU-S. In the group of animals given BU-S, toxic effects such as severe tachypnea, muscle spasm, arrhythmia and paralysis were observed in all the dose groups. All deaths occurred in the first 4 h. Animals that survived beyond 4 h appeared to improve and by 24 h were eating and behaving normally. At the dose of 3.24 mg/kg, all mice died after being injected with BU-S, but only five mice died in the BU-NLC group. There were no marked toxic effects evident in the experimental animals injected with BU-NLC at a dose of 1.32 mg/kg. These results demonstrated that the BU-NLC was less toxic than BU-S.

4. Discussion

From the biodistribution data, bufadienolides exhibited a relatively higher concentration in the brain, which suggested their use as a potential new approach to the treatment of brain cancer. Therefore, the cytotoxic effect of BU-NLC on U87-MG cells was assayed. The cytotoxicity of BU-NLC at 48 h was higher than that of BU-D, whereas at 72 and 96 h BU-NLC was less cytotoxic. The cytotoxicity of BU-NLC in the U87-MG cell line may be due to the bufadienolides release pattern exhibited by the formulation. The *in vitro* release study results (Li et al., 2010) showed that the drug release from BU-NLC fitted the Weibull distribution closely. The drug was released rapidly during the initial stage (8 h, 40%) and then exhibited by sustained release at a constant rate up to 120 h. The percentage cumulative release of bufadienolides was 85%. Thus, BU-NLC that entrapped drugs in its lipid matrix was able to reduce the cytotoxicity of bufadienolides. For the U87-MG cell line at 48 h, the cytotoxicity of bufadienolides was increased when incorporated in NLC. There were two possibilities to explain the mechanism of cytotoxicity for BU-NLC: (1) bufadienolides were released from BU-NLC outside the cells and acted like BU-D; (2) bufadienolides were carried by BU-NLC and released inside the cells, resulting in higher cytotoxicity. Therefore, after 48 h exposure, the fast internalization of BU-NLC enhanced the inhibitory activity of free bufadienolides outside the cell. At 72 and 96 h, the free bufadienolides outside the cell may exhibit their full cytotoxic activity. Taken together, these results show that the cytotoxicity of BU-NLC against the two cell lines was comparable with that of the free drug.

We previously reported (Zhang et al., 2008) a novel, rapid and specific ultra performance liquid chromatography tandem mass spectrometry method for simultaneous determination of three bufadienolides in rat plasma. In the present work, the method was successfully used to quantify bufadienolides in plasma and tissues samples in a pharmacokinetic and tissue distribution study of BU-NLC. After i.v. delivery of BU-NLC, the peak plasma concentration (C_{max}) and $AUC_{(0-\infty)}$ of B, C and R were markedly elevated ($P < 0.05$), and their CL was reduced ($P < 0.05$). This result was consistent with the literature reports of other scientists (Manjunath and Venkateswarlu, 2005; Jung et al., 2009). The main reason was the drug distribution in the preparation. NLC is a multiple system, being a solid lipid matrix. This solid lipid matrix (Wissing et al., 2004) contains tiny liquid oil nanocompartments. Thus, the drug solubility in oils is higher than its solubility in solid lipids. Our previous report (Li et al., 2010) indicated that the drug was completely solubilized in the lipid materials of the BU-NLC. The EEs of the bufadienolides were all above 85%. Little drug was distributed in the aqueous phase and direct contact of the drug with body fluids and tissues was avoided. Thus, NLC exhibited a markedly slower release. The second reason might be the hydrophilic surface of BU-NLC. It has been reported that copolymers, such as poloxamers and poloxamines, are typically very flexible and highly hydrophilic, which can help shield the charged particles from blood proteins (Owens and Peppas, 2006).

Cardioactivity is a unique characteristic of steroids such as bufadienolides (Bick et al., 2002; Krylov, 2002) and one goal of NLC formulation is to reduce exposure of the heart to the drug. Bufadienolides increased the contractility of cardiac muscle in a dose-dependent manner, just as digitalis does. According to one

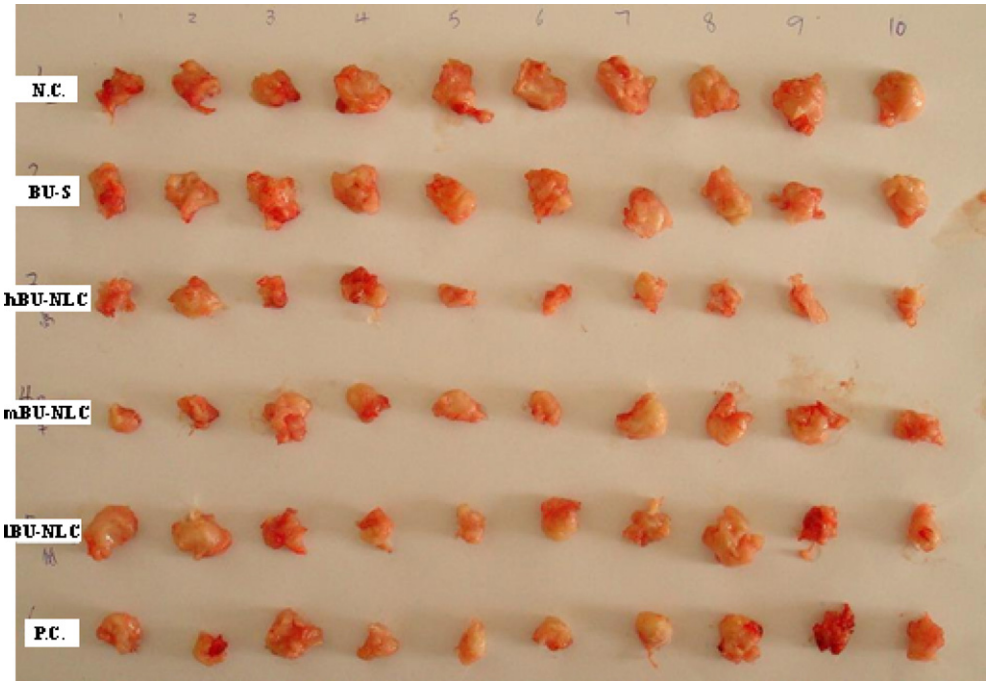

Fig. 6. S180 solid tumors stripped from each group.

report, a 24-year-old male died soon after an intravenous injection of toad extract (Kostakis and Byard, 2009). A trace of bufotenine at a level below the lowest calibrator of 1.8 ng/mL was present in blood sample from the deceased, but no bufadienolides were detected. This report agreed with our research showing that there was no detectable level of bufadienolides in heart 30 min after dosing. Bufadienolides do not have a cumulative nature *in vivo* (Shimizu and Morishita, 1996).

The distribution of B, C and R into the brain was increased with BU-NLC. According to earlier reports (Esposito et al., 2008), nanoparticles can open the tight junctions between endothelial cells in the brain microvasculature, thus creating a paracellular pathway for nanoparticle translocation. However, in the case of BU-S, in brain the concentrations of bufadienolides (especially C) were relative higher and they were metabolized slowly. The structural features of bufadienolides represent a type of steroid with an A/B cis and a C/D cis skeleton and an α-pyrone ring at the 17-position, which is similar to digitoxigenin. It was interesting to note that C and R have a unique epoxy group in their structure compared with B. In addition, there was an acetoxy group at the C-16 position of C. The log *P* values of B, C and R were all around 3. The higher lipophilicity, chemical structure and the low molecular weight below 400 Da (Kreuter, 2001) helped B, C and R to cross the blood–brain barrier, which largely controlled the clearance of particles from the blood. Therefore, the free bufadienolides which were not loaded into NLC could also be easily transported across brain endothelial cells by passive diffusion. This suggests a potential new approach to the treatment of brain cancer.

The *in vivo* antitumor study indicated that, compared with BU-S, BU-NLC exhibited a notably enhanced antitumor efficacy. This may be the fact that nanoparticles entrapped within the liver and spleen acted as a reservoir to gradually release the encapsulated drug (Soma et al., 2000). It was also helpful to maintain a certain systemic drug level. It is worth noting that tumor cells often exhibited enhanced endocytotic activity, leading to increased internalization of nanoparticles and drug release inside the tumor. The particles of BU-NLC might be internalized by endocytosis due to their mesoscopic size in the range of 20–200 nm, which enhanced the uptake of drug (Savić et al., 2003). Hence, taking into consideration the sustained release behavior of BU-NLC, a prolonged and continuous attack on tumor cells can be produced with the help of nanoparticles. On the other hand, compared with the P.C. group, bufadienolides enhanced the immunologic function of S180-tumor-bearing mice. This result confirmed that of a previous report (Terness et al., 2001) that bufadienolides were extremely potent T-cell suppressive agents, which represent an important bioregulatory link between the cardiovascular, nervous and immune systems.

In the safety study, the BU-NLC aqueous suspensions were non-haemolytic up to the tested concentration of 1.2 mg/mL. Although the LD_{50} of BU-NLC was only 1.28-fold higher than that of BU-S, BU-NLC exhibited a higher antitumor inhibition rate than BU-S (67.12% vs. 36.93%) at the same dose (1.0 mg/kg). Cardiac glycosides are drugs with a narrow therapeutic range. Taken together, the administration of BU-NLC at a lower dose was effective in inhibiting the growth of S180-tumors *in vivo* but did not produce a direct toxic effect. These results indicated that BU-NLC overcame the disadvantages of a solution of bufadienolides containing an organic solvent, appearing to be the best possible approach to by passing the limitations of cardiac toxicity and provide a desirable

Table 4
Hemolysis rates of BU-NLC at lipid concentrations of 3.0 and 1.2 mg/mL (each value represents the mean value ± S.D., $n = 3$).

Lipid concentration (mg/mL)	Hemolysis rates with different sample volumes (%)				
	0.1 mL	0.2 mL	0.3 mL	0.4 mL	0.5 mL
3.0	3.51 ± 0.73	5.77 ± 0.86	15.83 ± 2.76	36.86 ± 3.87	84.70 ± 5.38
1.2	0.55 ± 0.41	1.77 ± 0.48	2.22 ± 0.39	3.61 ± 0.66	4.30 ± 0.62

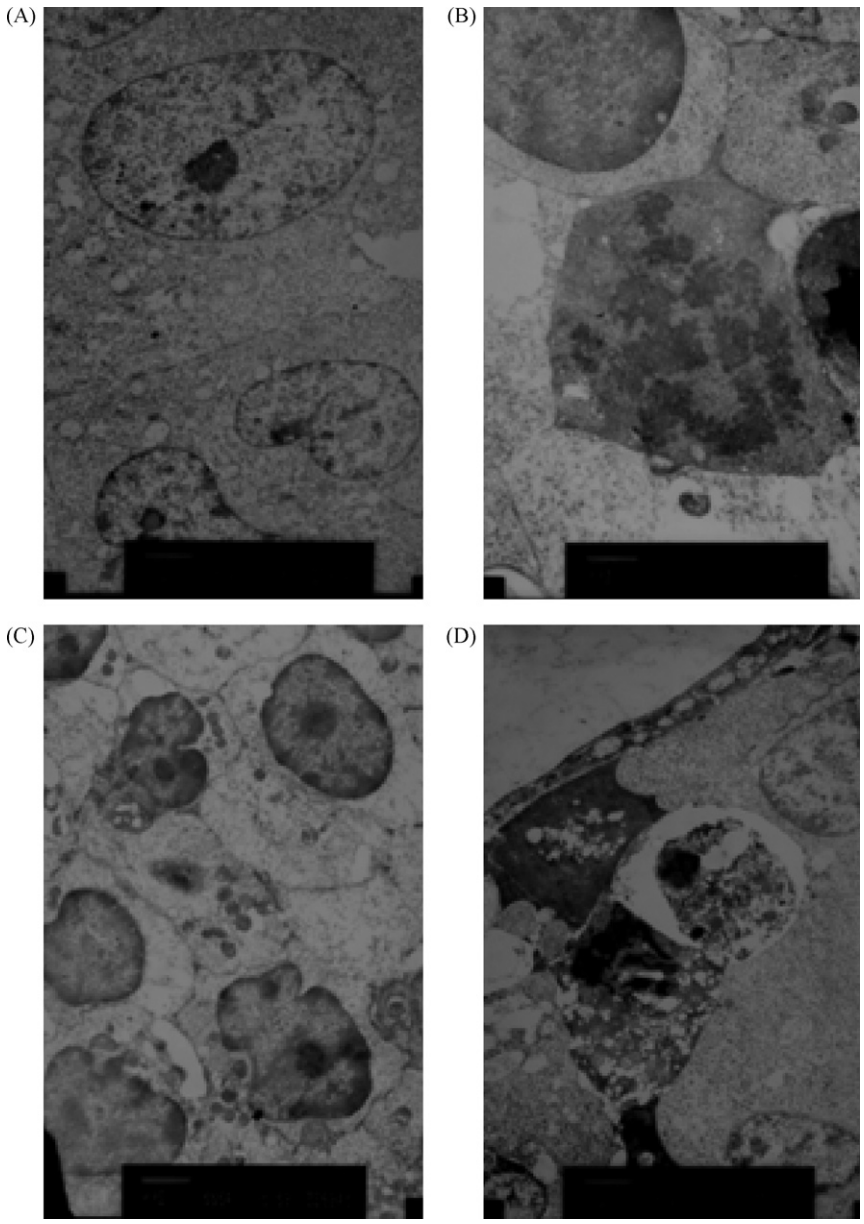

Fig. 7. Morphological changes of tumor S180 cells under transmission electron microscopy (4000× magnification). A: mice treated with normal saline; B: mice treated with BU-NLC at dosage of 1.0 mg/kg/d; C: mice treated with BU-S at dosage of 1.0 mg/kg/d; D: mice treated with cyclophosphamide.

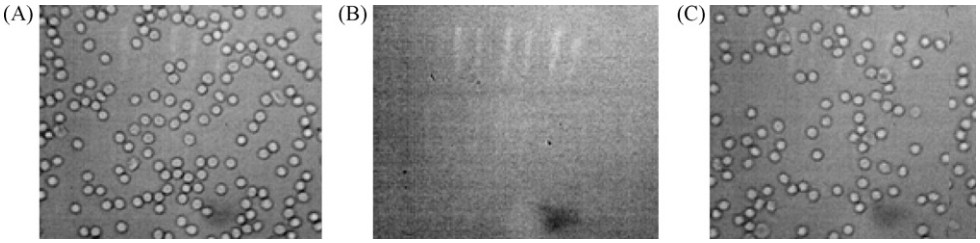

Fig. 8. Optical microscope photos of erythrocytes in each group under oil immersion. A: Erythrocytes of negative control; B: Erythrocytes of positive control; C: Erythrocytes of BU-NLC (at a lipid concentration of 1.2 mg/mL) incubated for 1 h.

therapeutic efficacy. In clinical practice, the combined application of the commercially available Huachansu injection and other chemotherapeutic drugs is an effective treatment of tumors (Qin et al., 2008). Therefore, an experimental study of the prevention of toxic effects at a high concentration bufadienolides could be conducted by combining BU-NLC and chemotherapeutic drugs to exert more beneficial effects.

5. Conclusion

This is the first report describing the *in vitro* cytotoxicity, pharmacokinetics, biodistribution, antitumor efficacy and safety of BU-NLC after intravenous administration. Cytotoxicity testing in U87-MG and HGC-27 cell lines showed that BU-NLC had a comparable cytotoxicity to the free drug. The *in vivo* study revealed that the

encapsulated bufadienolides in BU-NLC improved the pharmacokinetic parameters and biodistribution. On the whole, incorporation of bufadienolides in NLC reduced the adverse effects of a solution of bufadienolides, exhibited superior antitumor effect and good hemocompatibility. In conclusion, the NLC system is a promising approach for the intravenous delivery of bufadienolides. More detailed evaluation is needed to prove the efficacy in clinical applications and elucidate the mechanisms of the antitumor effect.

Acknowledgements

Dr. David B Jack is gratefully thanked for correcting the manuscript. The authors acknowledged X. Lin and Z.T. Liu for helping with ultra performance liquid chromatography tandem mass spectrometry analysis, L. Wei, S. Sha and G.X. Zang for helping with the antitumor experiment. These studies were supported by the Ministry of Science and Technology of the P.R. China (Grant 2009ZX09102-124) and the State Administration of Traditional Chinese Medicine of the P.R. China (Grant 06-07ZP04).

References

Abdel-Rahman, M.A., Ahmed, S.H., Nabil, Z.I., 2010. In vitro cardiotoxicity and mechanism of action of the Egyptian green toad Bufo viridis skin secretions. Toxicol. In Vitro 24, 480–485.

Bick, R.J., Poindexter, B.J., Sweney, R.R., Dasgupta, A., 2002. Effects of Chan Su, a traditional Chinese medicine, on the calcium transients of isolated cardiomyocytes: cardiotoxicity due to more than Na, K-ATPase blocking. Life Sci. 72, 699–709.

Couvreur, P., Vauthier, C., 2006. Nanotechnology: intelligent design to treat complex disease. Pharm. Res. 23, 1417–1450.

Esposito, E., Fantin, M., Marti, M., Drechsler, M., Paccamiccio, L., Mariani, P., Sivieri, E., Lain, F., Menegatti, E., Morari, M., Cortesi, R., 2008. Solid lipid nanoparticles as delivery systems for bromocriptine. Pharm. Res. 25, 1521–1530.

Fundarò, A., Cavalli, R., Bargoni, A., Vighetto, D., Zara, G.P., Gasco, M.R., 2000. Non-stealth and stealth solid lipid nanoparticles (SLN) carrying doxorubicin: pharmacokinetics and tissue distribution after i.v. administration to rats. Pharmacol. Res. 42, 337–343.

Joshi, M.D., Müller, R.H., 2009. Lipid nanoparticles for parenteral delivery of actives. Adv. Drug Deliv. Rev. 71, 161–172.

Junzo, S., Satoru, S., Akiira, S., 2004. A nanometer lipid emulsion, lipid nano-sphere (LNS), as a parenteral drug carrier for passive drug targeting. Int. J. Pharm. 273, 75–83.

Jung, S.H., Lim, D.H., Jung, S.H., Lee, J.E., Jeong, K.S., Seong, H., Shin, B.C., 2009. Amphotericin B-entrapping lipid nanoparticles and their in vitro and in vivo characteristics. Eur. J. Pharm. Sci. 37, 313–320.

Kamano, Y., Yamashita, A., Nogawa, T., Morita, H., Takeya, K., Itokawa, H., Segawa, T., Yukita, A., Saito, K., Katsuyama, M., Pettit, G.R., 2002. QSAR evaluation of the Chan Su and related bufadienolides against the colchicine-resistant primary liver carcinoma cell line PLC/PRF/51. J. Med. Chem. 45, 5440–5447.

Kostakis, C., Byard, R.W., 2009. Sudden death associated with intravenous injection of toad extract. Forensic Sci. Int. 188, e1–5.

Krenn, L., Kopp, B., 1998. Bufadienolides from animal and plant sources. Phytochemistry 48, 1–29.

Kreuter, J., 2001. Nanoparticulate systems for brain delivery of drugs. Adv. Drug Deliv. Rev. 47, 65–81.

Krylov, V.N., 2002. Study of cardiotonic effect of venom of the green toad Bufoviridis. J. Evol. Biochem. Physiol. 38, 223–228.

Li, F., Wang, T., He, H.B., Tang, X., 2008. The properties of bufadienolides-loaded nano-emulsion and submicro-emulsion during lyophilization. Int. J. Pharm. 349, 291–299.

Li, F., Wang, Y., Liu, Z., Lin, X., He, H., Tang, X., 2010. Formulation and characterization of bufadienolides-loaded nanostructured lipid carriers. Drug Dev. Ind. Pharm., doi:10.3109/03639040903264397.

Li, F., Yang, R., Weng, Y., Tang, X., 2009. Preparation and evaluation of lyophilized liposome-encapsulated bufadienolides. Drug Dev. Ind. Pharm. 35, 1048–1058.

Manjunath, K., Venkateswarlu, V., 2005. Pharmacokinetics, tissue distribution and bioavailability of clozapine solid lipid nanoparticles after intravenous and intraduodenal administration. J. Contr. Release 107, 215–228.

Miglietta, A., Cavalli, R., Bocca, C., Gabriel, L., Gasco, M.R., 2000. Cellular uptake and cytotoxicity of solid lipid nanospheres (SLN) incorporating doxorubicin or paclitaxel. Int. J. Pharm. 210, 61–67.

Müller, R.H., Rühl, D., Runge, S., Schulze-Forster, K., Mehnert, W., 1997. Cytotoxicity of solid lipid nanoparticles as a function of the lipid matrix and the surfactant. Pharm. Res. 14, 458–462.

Müller, R.H., Petersen, R.D., Hommoss, A., Pardeike, J., 2007. Nanostructured lipid carriers (NLC) in cosmetic dermal products. Adv. Drug Deliv. Rev. 59, 522–530.

Owens 3rd, D.E, Peppas, N.A., 2006. Opsonization, biodistration and pharmacokinetics of polymeric nanoparticles. Int. J. Pharm. 307, 93–102.

Qin, T.J., Zhao, X.H., Yun, J., Zhang, L.X., Ruan, Z.P., Pan, B.R., 2008. Efficacy and safety of gemcitabine-oxaliplatin combined with huachansu in patients with advanced gallbladder carcinoma. World J. Gastroenterol. 14, 5210–5216.

Savić, R., Luo, L., Eisenberg, A., Maysinger, D., 2003. Micellar nanocontainers distribute to defined cytoplasmic organelles. Science 300, 615–618.

Schubert, M.A., Harms, M., Müller-Goymann, C.C., 2006. Structural investigations on lipid nanoparticles containing high amounts of lecithin. Eur. J. Pharm. Sci. 27, 226–236.

Shimizu, Y., Morishita, S., 1996. Metabolism and disposition of kyushin, a drug containg senso (ch'an su). Am. J. Chin. Med. 24, 289–303.

Soma, C.E., Dubernet, C., Barratt, G., Benita, S., Couvreur, P., 2000. Investigation of the role of macrophages on the cytotoxicity of doxorubicin and doxorubicin-loaded nanoparticles on M5076 cells in vitro. J. Contr. Release 68, 283–289.

Steyn, P.S., van Heerden, F.R., 1998. Bufadienolides of plant and animal origin. Nat. Prod. Rep. 15, 397–413.

Terness, P., Navolan, D., Dufter, C., Kopp, B., Opelz, G., 2001. The T-cell suppressive effect of bufadienolides: structural requirements for their immunoregulatory activity. Int. Immunopharmacol. 1, 119–134.

Toma, S., Hirai, Y., Sugimoto, C., Shoji, M., Oguni, Y., Morishita, S., Ito, C., Horie, M., 1991. Metabolic fate of bufalin and cinobufagin. Yakugaku Zasshi 111, 687–694.

Wissing, S.A., Kayser, O., Müller, R.H., 2004. Solid lipid nanoparticles for parenteral drug delivery. Adv. Drug Deliv. Rev. 56, 1257–1272.

Yeh, J.Y., Huang, W.J., Kan, S.F., Wang, P.S., 2003. Effects of bufalin and cinobufagin on the proliferation of androgen dependent and independent prostate cancer cells. Prostate 54, 112–124.

Zhang, L.S., Yoshida, T., Aoki, K., Kuroiwa, Y., 1991. Metabolism of cinobufagin in rat liver microsomes. Identification of epimerized and deacetylated metabolites by liquid chromatography/mass spectrometry. Drug Metab. Dispos. 19, 917–919.

Zhang, Y., Tang, X., Liu, X.L., Li, F., Lin, X., 2008. Simultaneous determination of three bufadienolides in rat plasma after intravenous administration of bufadienolides extract by ultra performance liquid chromatography electrospray ionization tandem mass spectrometry. Anal. Chim. Acta 610, 224–231.